Available online at www.sciencedirect.com

ScienceDirect

Procedia Engineering 86 (2014) 223 – 233

Procedia Engineering

www.elsevier.com/locate/procedia

1st International Conference on Structural Integrity, ICONS-2014

Study on the Effect of Post Weld Heat Treatment Parameters on the Relaxation of Welding Residual Stresses in Electron Beam Welded P91 Steel Plates

K. Abburi Venkata[a,*], S. Kumar[b], H. C. Dey[c], D. J. Smith[a], P. J. Bouchard[d] and C. E. Truman[a]

[a]*Department of Mechanical Engineering, University of Bristol, Bristol, UK*
[b]*Bhabha Atomic Research Centre, Mumbai-400085, India*
[c]*Indira Gandhi Centre for Atomic Research, Kalpakkam-603102, India*
[d]*Materials Engineering, The Open University, Milton Keynes, UK*
[*]*E-mail ID: k.abburivenkata@bristol.ac.uk*

Abstract

Residual stresses are created by localised heating effects that occur during the welding process. Post weld heat treatment (PWHT) is the most convenient method for stress relief of welds. But PWHT cannot completely eliminate the residual stresses. So, it is essential to determine the influence of PWHT parameters like holding temperature and time on the stress relaxation for optimising the process. The selected material is modified 9Cr-1Mo (Grade 91) steel in the form of plates welded together using a high intensity electron beam. To facilitate the study, a numerical thermo-elastic-plastic model has been developed to simulate the welding of the plates. As P91 steels undergo phase transformations, the corresponding volumetric change and transformation plasticity are taken into consideration during the analysis and welding residual stresses are predicted. PWHT is implemented using Norton creep law and the residual stresses after relaxation are determined. The developed model and the predictions are validated using neutron diffraction measurements on as welded and post weld heat treated plates. A good agreement has been achieved between the measurements and predictions. The validated model has been used to study the effect of variation of heat treatment parameters like holding temperature and time on the relaxation of welding stresses.

Peer-review under responsibility of the Indira Gandhi Centre for Atomic Research

Keywords: Post weld heat treatment, holding time and temperature, phase transformations, residual stress, creep relaxation

1. Introduction

Welded joints are used extensively in construction, ship building, steel bridges, and pressure vessels and are often considered the weakest part in the component or assembly. The modified 9Cr-1Mo (Grade 91) is a

Peer-review under responsibility of the Indira Gandhi Centre for Atomic Research
doi:10.1016/j.proeng.2014.11.032

structural steel used extensively in pressure vessels and steam generators for the next generation power plants because of the desirable properties like high creep rupture strength and toughness at elevated temperatures. P91 steel undergoes phase transformation from austenite to martensite during rapid cooling. Electron beam welding is a fusion welding process in which the weld material reaches the material's melting point, creating localised residual stresses. These stresses affect the performance of welded structures and need to be removed. The residual stresses may decay during service but under creep conditions they may reduce the life expectancy of the component. If the weldment undergoes PWHT, the residual stresses can be relieved but not completely eliminated.

There is an extensive literature on the prediction of residual stresses after heat treatment. Yaghi et al [1] used an axi-symmetric model to simulate the welding and post weld heat treatment processes, and predict the residual stresses and the stress relaxation respectively. Hishashi et al [2] developed a numerical model to simulate the post weld heat treatment of electron beam welded joint in International Thermonuclear Experimental Reactor (ITER) test blanket module. Akbarzadeh et al [3] used experimental and numerical studies of post weld heat treatment to determine the effect of heat treatment parameters on the relaxation of welding residual stresses. Cho et al [4] implemented post weld heat treatment analysis on welding simulation of multi-pass welds to determine the residual stress state before and after the heat treatment and validated the predictions using hole-drilling measurement of the stresses. Philippe Bastid [12] from TWI has done a detailed post-weld heat treatment analysis using finite element modelling to predict the residual stresses in huge pipe connections after local PWHT. Through his analysis he emphasised the significance of applying an elastic model and an elastic-visco-plastic model to simulate PWHT. His work concluded that residual stresses were of higher magnitude using elastic models than that from elastic-visco-plastic analysis. Dong et al [13], used experiments as well as numerical analysis to study and understand the stress relief mechanism in PWHT. He observed that although the stress relief can occur from plastic deformation induced stress relief due to change in the yield strength of the material with temperature, the most dominant stress relief mechanism is creep strain induced stress relaxation.

In the present paper, a two-dimensional model was used to simulate the electron beam welding process on P91 steel plates using a coupled thermo-mechanical analysis to predict the residual stresses. The thermal analysis was implemented using transient heat transfer analysis and the residual stresses were simulated after taking into account the volume change due to phase transformations during and transformation plasticity. The predicted residual stresses were validated by neutron diffraction measurements. Post weld heat treatment simulation was implemented using a coupled thermo-mechanical analysis like the original weld analysis and the stress relaxation due to heat treatment was predicted. Also, the effects of the heat treatment parameters, the holding time and the holding temperature were studied with the aim of arriving at the optimised values for these parameters.

2. Welding Simulation

Welding involves high temperature thermal cycles at the joint resulting in highly non-linear thermal and mechanical behaviour due to temperature dependency of the material properties and boundary conditions. As a result it is impossible to solve the thermo-mechanical equations using analytical approach. Numerical methods, finite element method in particular is highly advantageous and useful in solving these complex equations.

The welding process was simulated using an uncoupled thermo-mechanical finite element analysis using ABAQUS. The transient thermal history predicted by the thermal analysis was applied to the mechanical analysis and the residual stresses were predicted. The complex mechanics involved in the phase transformation of the steel during the cooling phase were incorporated in the mechanical analysis using the Koinstinen-Marburger relationship [5]. The solid state phase transformation (SSPT) induces volumetric changes in the material affecting the final residual stress state. Throughout the analysis various user-subroutines such as DFLUX and UEXPAN were used to model the shape of the heat source and the phase transformations.

2.1 Analysis Procedure

A two-dimensional model was used to model the geometry of the cross-section of the plates as shown in Fig. 1. It is assumed that the centre of the plate during the welding is at steady-state unlike the start and the stop ends where the heat flow is transient. As a result, a cross-section at the centre of the plate can be used effectively to

model the residual stresses with reasonable likeness to the actual stress-state in the three-dimensional plate. The plates were made of modified P91 steel whose chemical composition is given below in Table 1 and joined together using electron beam welding. The welding parameters were tabulated in Table 2. The plates were arranged in a butt weld configuration with a gap between the parting surfaces less than 100 μm. The plates were clamped to a heavy base plate with a blind square groove beneath the weld line. Spot welds were made along the length of the plate at three locations to assist the welding. But they were not modelled in the analysis. The weld was very narrow with a fusion zone (FZ) width of approximately 1.2 mm and a heat affected zone (HAZ) width of 0.7 mm.

Table 1. Chemical composition of the steel (wt. %) (Balance Fe)

C	Mn	Zr	Si	P	S	Cr	Mo	Ni	Cu	Al	N	Nb	Ti	V
0.106	0.443	0.005	0.221	0.018	0.0008	8.965	0.901	0.212	0.045	0.010	0.0464	0.073	0.004	0.194

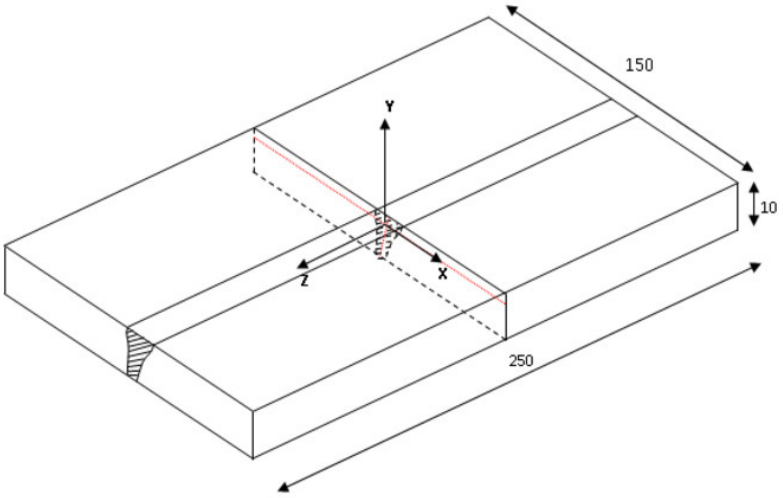

Figure 1. Electron beam welded P91 plate and the cross-section of the model

Table 2. Welding process parameters

Process	Beads	Power (KW)	Speed (m/min)
EBW	One pass weld	4.2	1

2.2 Thermal Analysis

The heating of the welding plates and the subsequent cooling was modelled in the thermal analysis to simulate the actual welding process. Equation (1) is the differential equation for the heat transfer given as:

$$\frac{\partial}{\partial x}\left(k\frac{\partial T}{\partial x}\right)+\frac{\partial}{\partial y}\left(k\frac{\partial T}{\partial y}\right)+\frac{\partial}{\partial z}\left(k\frac{\partial T}{\partial z}\right)=\rho C\frac{\partial T}{\partial t} \quad [1]$$

where T(x, y, z, t) is the current temperature, ρ is the density and C is the specific heat, t is the time and k is the thermal conductivity. As the specific heat and thermal conductivity are temperature dependent, the eq. (1) becomes non-linear. To simulate the heating of the plates, a moving heat source in the shape of a cone and a double ellipsoid was modelled using the user-subroutine DFLUX. The volumetric heat source is given by [2]

$$DFLUX = \eta\frac{UI}{V} \quad [2]$$

where U is the voltage, I is the current, η is the efficiency and V is the weld pass volume. The conical heat source is defined using 2 halves. The frontal part is modelled using the eq. (3) [6] as:

$$q_{f(x,y,z)} = \frac{6f_f Q}{abc_f \pi(1+d_c)} e^{-3\frac{x^2}{a^2}}\left(1 - \frac{(1-d_c)|y|}{b}\right)e^{-3\frac{z^2}{c_f^2}} \quad [3]$$

The rear part is modelled using eq. (4) [6] as:

$$q_{r(x,y,z)} = \frac{6f_r Q}{abc_r \pi(1+d_c)} e^{-3\frac{x^2}{a^2}}\left(1 - \frac{(1-d_c)|y|}{b}\right)e^{-3\frac{z^2}{c_r^2}} \quad [4]$$

where a, b, c_f and c_r are the semi axes in the X, Y, and Z directions respectively, Q is the total heat input. The parameter d_c ranges between 0 and 1, to decrease the diameter of the cone, through the depth. The frontal part of the double ellipsoid is defined using the eq. (5) [6] as:

$$q_{e(x,y,z)} = \frac{6\sqrt{3}f_f Q}{abc_r \pi^{\frac{3}{2}}} e^{-3\frac{x^2}{a^2}} e^{-3\frac{y^2}{b^2}} e^{-3\frac{z^2}{c_f^2}} \quad [5]$$

The rear part is modelled using eq. (6) [6] as:

$$q_{e(x,y,z)} = \frac{6\sqrt{3}f_f Q}{abc_r \pi^{\frac{3}{2}}} e^{-3\frac{x^2}{a^2}} e^{-3\frac{y^2}{b^2}} e^{-3\frac{z^2}{c_r^2}} \quad [6]$$

The finite element mesh is shown in Fig. 2. The first order heat transfer brick elements were used for the thermal analysis. The thermal properties such as thermal conductivity, specific heat, used in the analysis were taken as temperature dependent and are shown in Fig. 3. Density is taken as a constant. The latent heat effects were incorporated in the analysis. The thermal boundary conditions were taken into consideration by allowing for radiation heat transfer as electron beam welding was made in vacuum. The welding efficiency was assumed as 90%.

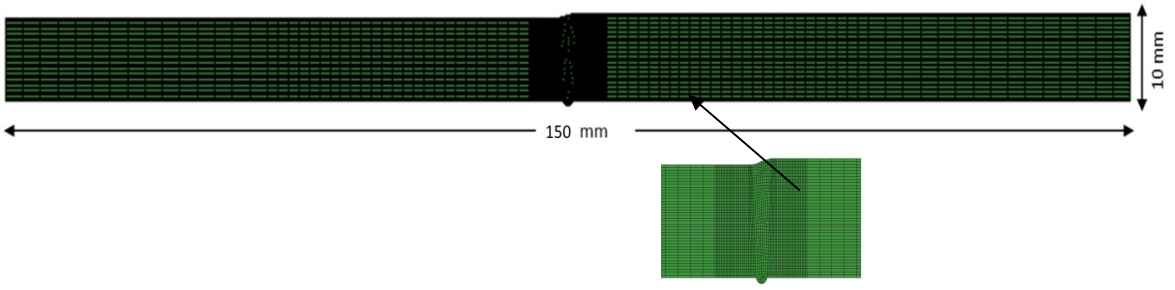

Figure 2. Finite element mesh with exploded view

2.3 Phase Transformations

Modified P91 steel exhibits solid-state phase transformation during rapid cooling, resulting in volumetric change. The volumetric change during heating and cooling is taken from the thermal dilation curve shown in Fig. 4. The experimental details for generating the dilation curve are published elsewhere [11]. During cooling, there is a contraction of the steel until it reaches M_s (martensite start temperature) (375°C). The steel then starts to expand as it changes from bcc to bct (SSPT), until M_f (martensite finish temperature) (280°C). This transformation is displacive but not diffusive as the chemical composition of the steel does not change. In order to take this transformation related volumetric change into account, a user subroutine UEXPAN was used to change the thermal expansion coefficient relative to the volumetric change, dynamically based on the temperature and the martensite fraction in the weld. The martensite fraction can be calculated using Koistinen-Marburger relationship [1, 5, 7-8] given by the eq. (7) as:

$$f_m = 1 - e^{-0.011(M_s - T)} \; (T \leq M_s) \quad [7]$$

where f_m is the fraction of martensite at the current temperature T during cooling. The differential equation for the above eq. (8) can be given as:

$$\Delta f_m = \left\{-0.011 e^{0.011(T-M_s)}\right\} \Delta T \quad (T \leq M_s) \quad [8]$$

where ΔT is the temperature increment during cooling. The martensitic transformation also induces transformation plasticity due to the displacive nature [1, 7]. The yield strength of the material was reduced by 30 MPa using an appropriate user subroutine to capture the effects of transformation induced plasticity.

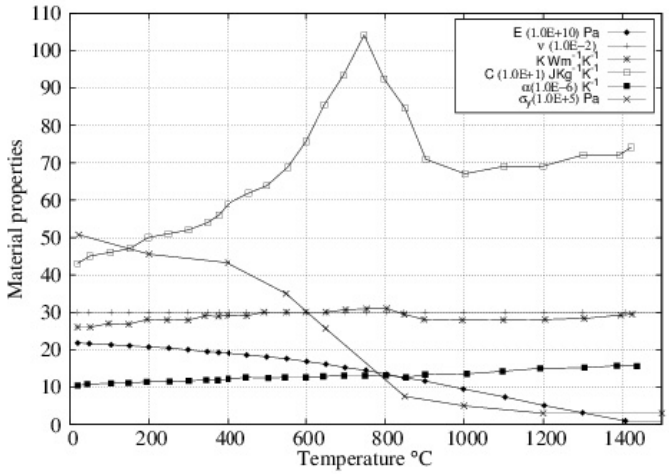

Figure 3. Material properties for P91 steel [1, 7]

2.4 *Structural Analysis*

The transient thermal history predicted in the thermal analysis was applied as a predefined field to the structural analysis to calculate the residual stresses. The FE structural analysis used the exact mesh as the thermal analysis. The total strain rate can be written as the sum of the individual components of the strain rate as:

$$\Delta\varepsilon = \Delta\varepsilon^{E} + \Delta\varepsilon^{P} + \Delta\varepsilon^{T} + \Delta\varepsilon^{\Delta V} + \Delta\varepsilon^{\Delta TR} \quad [9]$$

where $\Delta\varepsilon^{E}$, $\Delta\varepsilon^{P}$, $\Delta\varepsilon^{T}$, $\Delta\varepsilon^{\Delta V}$, $\Delta\varepsilon^{\Delta TR}$ is the strain due to elastic, plastic, thermal loading, volumetric change and transformation plasticity respectively. The material properties used for the analysis are the elastic modulus, the yield stress, Poisson's ratio and the linear thermal expansion coefficient. The material properties were considered to be temperature dependent. The hardening model was taken as Isotropic with annealing at 1050°C. First order plane strain elements with reduced integration were used as the mesh elements. The boundary conditions were used to a minimum extent to restrain the degrees of freedom of the plate. The plates were clamped heavily on the top during actual welding process to avoid distortion. This was also modelled in the analysis. The residual stresses were predicted as an output.

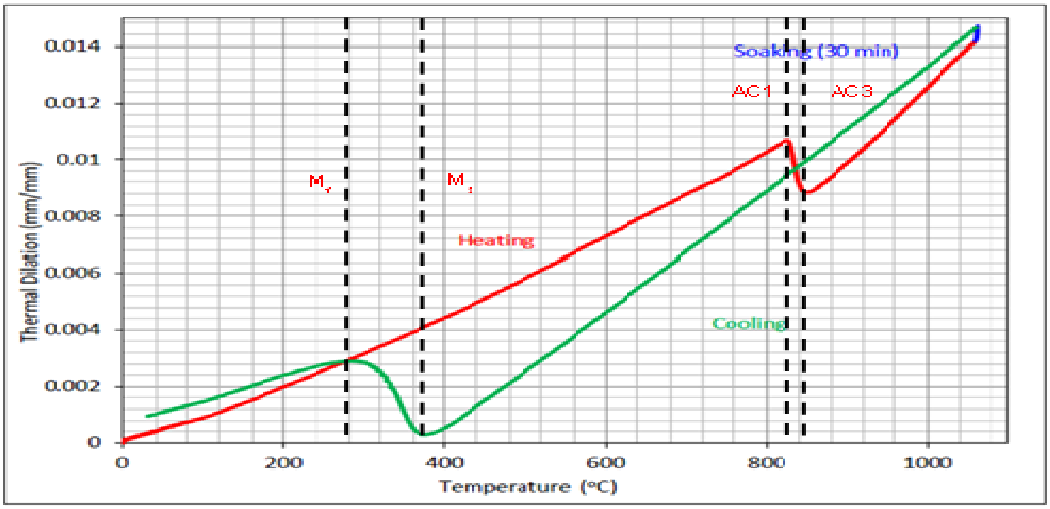

Figure 4. Measured thermal dilation of ASTM A387 Grade 91 steel [11]

2.5 Post-Weld Heat Treatment

The predicted welding residual stresses from the mechanical analysis were used as the input data for the post-weld heat treatment (PWHT) simulation. An uncoupled thermo-mechanical analysis was performed to model the post-weld heat treatment and predict the stress relaxation [3]. The stress relaxation occurs through two different phenomena, firstly due to the reduction of the yield strength with heating by using temperature dependent material properties and secondly the creep behaviour using Norton creep law to fit the secondary creep data. The numerical simulation of PWHT can be achieved by using temperature dependent material properties during the heating and cooling steps and by creep behaviour during the holding time. The Norton creep law used to model the creep behaviour is shown in eq. (10) as:

$$\dot{\varepsilon_c} = A\sigma^n \quad [10]$$

where $\dot{\varepsilon_c}$ is creep strain rate, A and n are temperature dependent coefficients, σ is the stress. As P91 steel undergoes phase transformation above austenite start temperature (AC1, ~825°C), PWHT temperature was maintained at 770°C and kept constant during the holding time. The sample is uniformly heated to the required temperature of 770°C for half an hour and then held at this temperature for an hour and half. The sample is cooled then at a controlled rate until the temperature drops to 400°C, after which the plate is cooled to room temperature. For the purpose of the analysis, it is essential to get the holding stage and the controlled cooling stage accurately modelled. Hence emphasis has been laid towards simulating these two stages accurately. The thermal cycle used in the simulation of PWHT process is shown in Fig. 5.

The values of A and n for P91 steel are not available for the temperature 770°C. So, the values were linearly extrapolated from known values at temperature 650°C. The extrapolation methodology is taken from the literature [1, 3, 8]. Once the stress relaxation has been simulated successfully, the same model was then used to investigate the effects of holding time and temperature on the stress relaxation, by running a series of PWHT analyses. The values of A and n were extrapolated according to the holding temperatures.

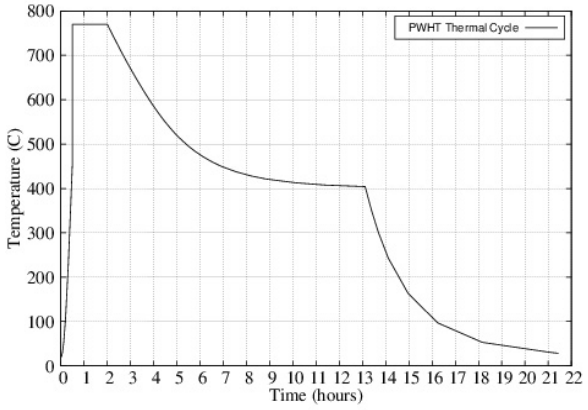

Figure 5. PWHT thermal cycle

3. Results and Discussion

3.1 Thermal Analysis

The thermal analysis predicted the fusion boundary with the temperature isotherms and also the thermal transient history and the peak nodal temperatures. The predicted fusion boundary and the temperatures are shown below. Figure 6(a) shows the predicted fusion boundary with the melted area and the HAZ. The cross sectional weld macrograph depicting the fusion boundary is shown in Fig. 6(b).

The validation of thermal analysis can be done by comparing the temperatures at different regions across the fusion and HAZ regions. But since there are no experimental measurements available during the welding procedure, the temperatures cannot be compared. An alternate way to comparing the temperatures is to compare the predicted isotherms with the regions from the macrograph. A detailed study of the macrograph has revealed that the fusion zone is 1.2 mm and the HAZ is approximately 0.7 mm. The grey region in the predicted fusion zone shown in Fig. 6(a) is approximately 1 mm, and the temperature in this region is above 1500 °C, indicating melting region. It can be observed that the predicted weld fusion area matches well with the actual fusion zone shown in the macrograph. At the HAZ/parent boundary, lies the inter-critical HAZ (ICHAZ) where the peak temperatures are between the critical temperatures AC1 (Austenite start temperature) and AC3 (Austenite finish temperature). From the dilation curve shown in Fig. 4, these values were marked as 825 °C and 865 °C. The predicted temperatures at these locations are exactly in the inter-critical temperature range, thereby predicted the extent of the HAZ region accurately. It is essential to get the extent of these zones right, in order to reliably predict residual stresses in the mechanical analysis. The extent of these zones in turn indicates the temperature experienced by each region, which in turn affects the residual stress distribution. Based on these comparisons it can be agreed that the thermal analysis has been validated with measured fusion boundary profile and that the predicted fusion boundary matches agreeably with that of the weld macrograph.

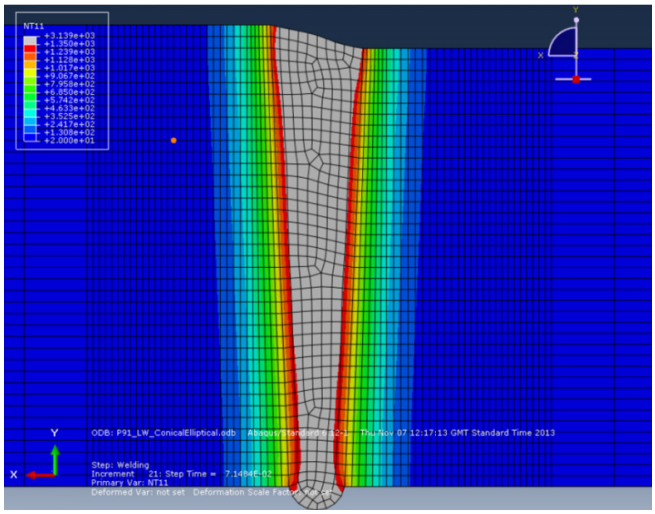

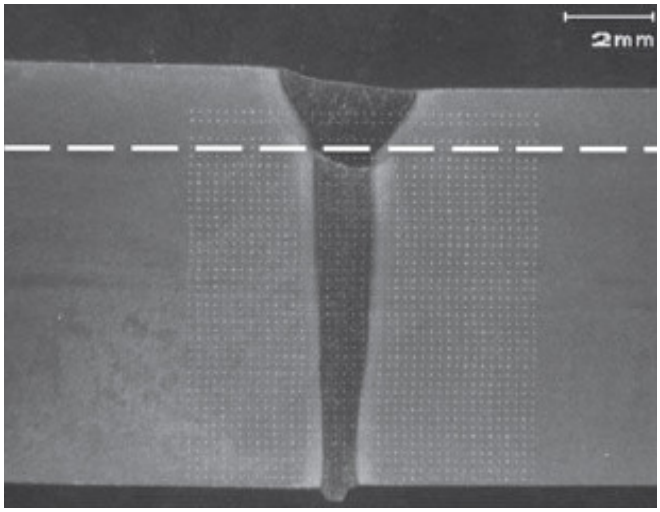

Figure 6(a). Predicted weld fusion zone 6(b). Weld macrograph

3.2 Mechanical Analysis

The mechanical analysis predicted the residual stresses by using the thermal field generated by the thermal analysis. Figure 7 shows the comparison of the predicted residual stresses developed due to welding with those of measured residual stresses using neutron diffraction measurements. The detailed description of the neutron diffraction experiment and the results are published elsewhere and are not discussed here [10]. The graph shows the longitudinal stresses across the weld at the depth of 1.5 mm from the top surface. It can be observed from the graph that the predictions and the measurements show a compressive stress or a near-zero stress at the weld centre and that the peak stresses are pushed into the parent region adjacent to the ICHAZ. This can be explained as a direct effect from the thermal dilation experienced during cooling stage.

The graph shows a characteristic 'M' shape predicted by the analysis, which is expected for a ferritic-martensitic steel undergoing phase transformation. It is essential to capture this variation in the residual stress spread which is in contrast to the trend observed in welding of austenitic steels. This emphasises the need to incorporate the effects phase transformation in the mechanical analysis to predict the residual stresses accurately. The measurements also show a compressive or a zero stress region at the centre of the weld, showing that the influence of thermal dilation and the volume change is significant. Also the result from an analysis without phase transformations is included in the comparison to show the significance of these on the final residual stress distribution. The longitudinal stress without phase transformation shows a peak tensile stress at the weld centre whereas the one with phase transformations shows a compressive stress.

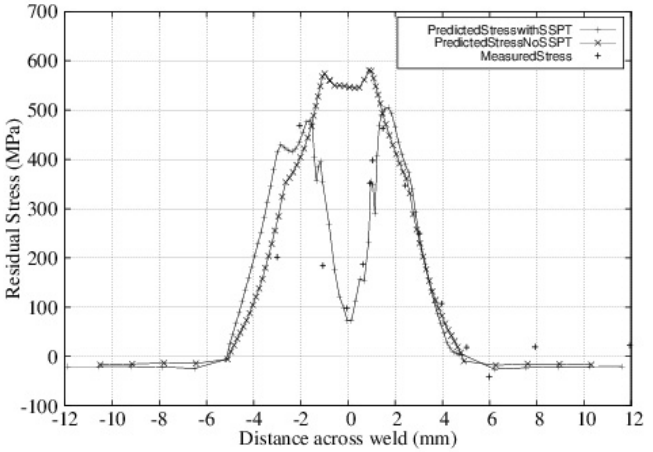

Figure 7. Comparison between predicted and measurement stresses

The slight variation in the predicted residual stress with that of measured values can be attributed to the various assumptions made in the mechanical analysis. Conventionally isotropic hardening is known to over-predict the residual stresses due to its conservative nature. This can be observed in the results very clearly. The model is a two dimensional approximation of a highly tri-axial problem, which might lead to some variations in the predictions compared to the measurements. It can be observed clearly that apart from these slight variations, the predicted residual stresses match favourably with the measurements from neutron diffraction experiment.

3.3 PWHT Analysis

The PWHT simulation resulted in the relaxation of residual stresses that are shown in Fig. 8. The As-Welded and PWHT residual stresses are shown in the same figure and it can be observed that the peak stresses are

reduced from 520 MPa to 170 MPa. The predictions show considerably higher stresses even after the relaxation. One possible reason could be due to the extrapolation of creep data, the constants A and n, for the required temperatures as there is no data available from experiments at the required temperature. But nevertheless the effect of stress relaxation due to heat treatment can be clearly seen. This relaxation is assumed to be arising from two different factors, one of it being the yield strength reduction at higher temperatures and the other from the creep strain development during the holding stage [13].

It is of interest to understand the influence of the post-weld heat treatment parameters on the stress relaxation in order to optimise the heat treatment process. The two parameters significantly affecting the heat treatment process are the holding time and the holding temperature. The effect of the holding time and the holding temperature on the relaxation of residual stresses is shown in Fig. 9(a) and 9(b). To study the effect of holding time on the residual stress relaxation, the holding temperature has been kept constant at 770°C and the holding time is varied. The effect of changing the holding time is shown in Fig. 9(a). It can be observed that changing the holding time from less than 1 hour to about 2 hours affects the residual stress relaxation to a higher extent than above 2 hours. The analysis was then used to predict the residual stresses at temperatures 770°C, 650°C and 550°C keeping the holding time constant at 1.5 hours. The residual stresses are shown in Fig. 9(b). It can be clearly seen from the graphs that the residual stresses are relaxed to a higher extent with the increase in holding temperature. The influence of holding temperature being considerably higher than the holding time can be explained from the creep behaviour simulated during the holding stage. The influence of temperature on the creep parameters and the creep strain is higher than that of time. The same can be observed in the results as well. The increase in the holding temperature has resulted in more creep strain induced stress relaxation which is the dominant stress relief mechanism.

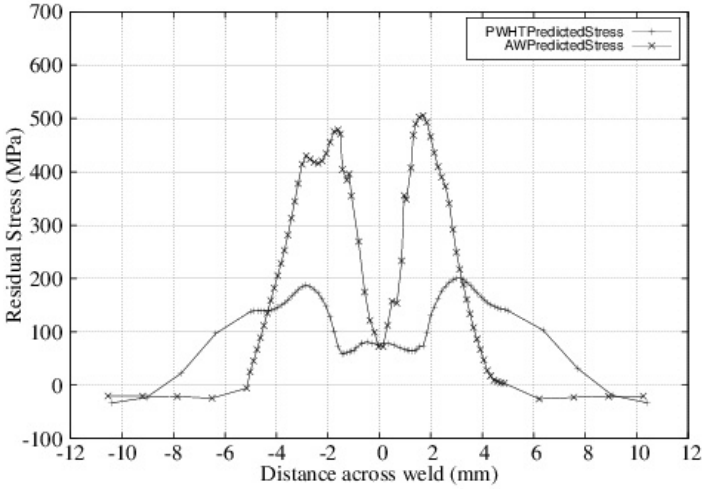

Figure 8. Predicted residual stress before and after PWHT

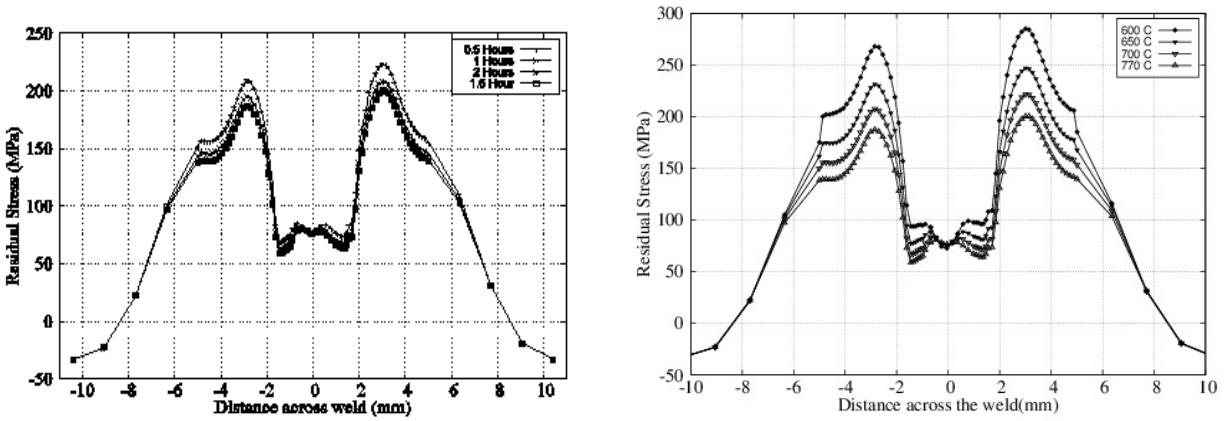

Figure 9. Effect of (a) holding time (b) holding temperature on residual stress relaxation

4. Conclusions

In this paper, the finite element simulations of electron beam welding process and PWHT for ferritic martensitic steel that undergoes phase transformations were performed. The residual stress predictions were validated using neutron diffraction measurements.

1. The thermal analysis used DFLUX subroutine to model the shape of the heat source and the transient thermal history is predicted. The structural analysis used the thermal history as the thermal loading to predict the residual stresses.
2. Stress relaxation due to PWHT was modelled using another coupled thermal and mechanical analysis. The mechanical analysis used elastic-visco-plastic model to simulate stress relaxation induced from plastic deformation as well as creep strain. The analysis has resulted in reduced residual stresses at the end of the cooling.
3. The effects of holding time and holding temperature were analysed and evaluated using the model. The effect of holding time was investigated using a constant holding temperature and it has been observed that the holding time is significant only up to the two hours. After that no significant relaxation can be achieved.
4. The effect of holding temperature was investigated for a constant holding time. The holding temperature is a very significant factor in the relaxation rate. Higher the holding temperature, greater is the relaxation of the residual stress. The maximum temperature that can be used is 770 ^{o}C and should definitely be less than AC1 (Austenite start temperature).

References

1. A. H. Yaghi et al., J. Strain Analysis, Vol.43 (2008) p 275.
2. H. Serizawa et al., J. Nucl. Mater. (2013), http://dx.doi.org/10.1016/j.jnucmat.2012.12.051
3. I. Akbarzadeh et al., J. Strain Analysis, Vol.46, (2010) p 79.
4. J. R. Cho et al., J. Materials Processing Technology (2004) p 1690.
5. Deng Dean, Murakawa Hidekazu, Computational Materials Science (2006) p 209.
6. A. Lundback, Mathematical modelling of Weld Phenomena 6 (2002) p 1113.
7. K. Abburi Venkata, Proceedings of the ASME 2013 Pressure Vessels & Piping Division Conference (2013)
8. A. H. Yaghi et al., J. Pressure Vessel Technology, Vol. 132 (2010), p 011206-1.
9. A. Lundback, Science and Technology of Welding and Joining, Vol. 10 (2005) p. 717
10. A Kundu, K A Venkata et al., Science and Technology of Welding & Joining, Vol. 18, Issue 1, pp. 70

11. S Kumar, K A Venkata et al., Materials Science and Engineering A, 575 (2013) p. 160
12. Philippe Bastid, TWI Member Publication, TWI CRP Report No 13837.01/02/1162.02, July 2013.
13. Dong P, et al., J. Pressure Vessels and Piping, 2014, p 1.